Phys. Med. Biol. **45** (2000) 49–58. Printed in the UK PII: S0031-9155(00)03092-X

# On the optimal energy of epithermal neutron beams for BNCT

E Bisceglie†, P Colangelo†, N Colonna†, P Santorelli‡ and V Variale†
† Istituto Nazionale di Fisica Nucleare, Sezione di Bari, 70123 Bari, Italy
‡ Dipartimento di Scienze Fisiche, Universitá Federico II e INFN, 80125 Napoli, Italy

Received 29 March 1999, in final form 28 September 1999

**Abstract.** The optimal neutron energy for the treatment of deep-seated tumours using boron neutron capture therapy is studied by analysing various figures of merit. In particular, analysis of the therapeutic gain as a function of the neutron energy indicates that, with the currently available $^{10}$B carriers, the most useful neutrons for the treatment of deep-seated tumours, in particular glioblastoma multiforme, are those with an energy of a few keV. Based on the results of the simulations, a method is presented which allows us to evaluate the quality of epithermal neutron beams of known energy spectrum, thus allowing us to compare different neutron-producing reactions and beam-shaping assembly configurations used for accelerator-based neutron sources.

## 1. Introduction

Boron neutron capture therapy (BNCT), a two-component modality for cancer treatment, relies on the use of neutron beams of suitable intensity and spectral features (for a recent review, see Barth *et al* (1996)). In particular, although the boron capture reaction occurs with thermal neutrons, the treatment of deep-seated tumours, such as glioblastoma multiforme (GBM), requires beams of neutrons of higher energy, that can penetrate more deeply into the tissues and thermalize in the proximity of the tumour region. The dose from proton recoil associated with fast neutrons, however, poses some constraints on the maximum neutron energy that can be tolerated in the treatment. For this reason, neutrons in the epithermal energy range, i.e. between 1 eV and 10 keV, are generally believed to be the most appropriate for the treatment of deep-seated tumours.

While the advantage of epithermal neutrons with respect to thermal ones is widely recognized, the optimal spectral features of the treatment beam are still the subject of debate. This aspect is particularly important in view of the present perspectives of using accelerator-based facilities to produce therapeutic beams, whose energy profile can be optimized by an appropriate choice of the neutron-producing reaction as well as of the material and geometry of the beam shaping assembly (BSA). Although the efficacy of the therapy depends on several factors, in particular on the ability to accumulate high concentrations of boron compound in the tumour, it is nevertheless fundamental to understand the optimal energy of the neutron beam, since a higher efficacy may result from an optimized neutron beam even with the currently available boron compounds (Wheeler *et al* 1999). Furthermore, while more efficient compounds would clearly lead to significant improvements in the delivered dose, the full advantage of such hypothetical compounds would not be realized without an optimized neutron beam.

0031-9155/00/010049+10$30.00  

With the aim of identifying the optimal spectral features of the neutron beams for BNCT, we have performed simulations of the dose deposition in the brain for monoenergetic neutrons, and we have analysed some significant figures of merit over a wide energy range. In particular, some implications for the optimal neutron energy for BNCT of deep-seated tumours can be drawn from the analysis of the therapeutic gain as a function of the neutron energy. The results of the simulations have inspired a method that allows us to evaluate the quality of realistic epithermal neutron beams of known energy profile, thus making it possible to perform fast and meaningful systematic studies of different neutron-producing reactions and various BSA configurations (moderator, reflector, filter), necessary to design and set up therapeutic neutron beams of the desired characteristics.

The paper is organized as follows: in section 2 we describe the Monte Carlo code used for the simulations, and present the results for monoenergetic and unidirectional neutron beams of given energy. In section 3 we analyse different figures of merit and discuss in particular the dependence of the therapeutic gain as a function of the neutron energy. In section 4 we describe a method for a fast evaluation of the beam quality, and compare the results with a complete simulation of the depth-dose distribution for some therapeutic neutron beams currently used or under consideration. Conclusions are drawn in section 5.

## 2. Monte Carlo simulations

Because of the nature of neutron interactions, BNCT analyses rely heavily on the use of Monte Carlo simulations. Calculations are necessary to predict the distribution of the dose released in the brain by a neutron beam of a known energy profile (Yanch *et al* 1991, Nigg 1994, Zamenhof *et al* 1996). More often, combined simulations of the moderation and dose deposition processes are performed to determine the beam-shaping assembly configuration, in particular the moderator material and its thickness, that would lead to the highest therapeutic effect for reactor (Aizawa 1994, Konijnenberg *et al* 1995, Liu *et al* 1996) or for accelerator-based neutron sources (Allen *et al* 1999, Bleuel *et al* 1998, Allen and Beynon 1995). Few attempts, however, have been made to identify *a priori* the optimal spectral features of the therapeutic neutron beam in the treatment of deep-seated tumours. Among such attempts, Wallace *et al* (1994) have shown the advantages of using an epithermal neutron beam with respect to a thermal one. This conclusion was based on the comparison between the dose distribution produced by a monoenergetic neutron beam of 35 eV and the one resulting from a thermal beam.

In this work, we have extended the analysis of Wallace *et al* (1994) to higher neutron energies, with the aim of better characterizing the optimal energy for the therapy. While most of the simulations of the dose distribution in BNCT have been obtained using an MCNP simulation code (Briesmeister 1993), we have followed a slightly different approach for the calculations of the dose delivered by neutrons in biological tissues. In this work, we have employed a code based on the simulation tool GEANT (Brun *et al* 1986) developed at CERN. In this package, neutron interactions are simulated by the MICAP routines developed at Oak Ridge National Laboratory (Johnson and Gabriel 1988). Similarly to the MCNP code, MICAP solves the Boltzmann transport equation using detailed energy and angular data from the ENDF/B database. The probability and the results of the interaction are determined according to cross sections that mirror the ENDF/B-6.1 data within a prescribed tolerance. In the simulation, each neutron is followed until it either disappears, due to a nuclear interaction or decay, or it reaches the boundary of a previously defined volume (in our case, a box of 1 $m^3$ dimension, containing the software replica of the head). All secondary neutrons and $\gamma$-rays resulting from the interactions are followed in the same way. Secondary charged particles are also followed,

with their energy loss determined in a quasi-continuum fashion according to calculated and tabulated stopping powers.

The code has been chosen for its versatility in the definition of materials and geometry, for the speed of computing, and for the possibility to run on virtually any machine and operating system. The most important feature of this kind of simulation, however, consists of the possibility of explicitly calculating the dose distribution starting from the energy released in the tissues by the secondary charged particles produced by neutron and $\gamma$ interactions, whereas in different codes the dose produced by the neutron beam is calculated employing appropriate kerma factors. In particular, assuming specific concentrations of $^{10}$B for both normal and tumour tissues, the boron capture reactions can be explicitly considered, and the products of the subsequent decay can be followed.

To check the consistency of our approach, we have compared the results of our simulations with calculations performed using the MCNP code. In particular, we have chosen as reference the work of Wallace *et al* (1994). For a meaningful comparison, we have performed simulations under the same conditions, by considering the same model of the skull and brain, with a tumour region of thickness 1 cm positioned at a depth of 5 cm from the brain surface. In our calculations, however, the $^{10}$B is explicitly included in the tissue composition, in concentrations of 10 and 43 parts per million (ppm) in healthy and tumour tissues respectively. In the subsequent analysis of the dose distribution, different concentrations in blood are also simulated by scaling the $^{10}$B capture dose by a corresponding factor, while keeping constant the ratio of blood/tumour $^{10}$B concentrations to 4.3 (this ratio, typical of *p*-boronophenylalanine, BPA, was assumed by Wallace *et al* (1994), and we use it to perform meaningful comparison with their results). As in the work by Wallace *et al* (1994), RBE factors of 1.6 and 2.3 for protons and $^{10}$B reactions respectively were considered in the dose analysis, although different RBE factors are currently being considered, in particular for $^{10}$B capture-related particles (Coderre and Morris 1999). It should be noted, however, that a different RBE factor is equivalent to a different $^{10}$B concentration in blood. Therefore, the general conclusions of this work, shown later for a range of concentrations, may be considered valid also for a different range of RBE values, such as those employed more recently.

The dose is calculated in elementary volumes of 0.25 cm side, directly from the energy released by the charge products of neutron and photon interaction. A unidirectional neutron beam of diameter 18 cm is generated and propagated through the software model of the head. Runs of 100 000 events take approximately 17 CPU minutes on an Digital Alpha 4000 workstation, with VMS operating system.

Figure 1 shows the results of the GEANT calculation for monoenergetic and unidirectional neutron beams at energies of 35 eV and 4 keV. The good agreement between the dose distribution at 35 eV, computed with GEANT, and that reported by Wallace *et al* (1994) confirms the correctness of the present approach (the agreement can be appreciated by comparing panel (*a*) of figure 1 with figure 4 of Wallace *et al* (1994); the difference between the two distributions, at the level of a few per cent, is within the statistical fluctuations). In the figure, the total dose is shown together with the various contributing components and with the results of a polynomial fit, described later. The comparison between the two different energies indicates that a larger number of thermal neutrons reach deeply into the tissues when the energy is increased up to a few keV, as is evident from the location of the maximum of capture-related doses. However, the increase of the dose released on the skin and brain surface by recoil protons, also evident from the comparison, becomes a limiting factor in the neutron energy. Therefore, a compromise has to be established between the need for more deeply penetrating neutrons and the requirement of keeping the surface dose to a tolerable level.

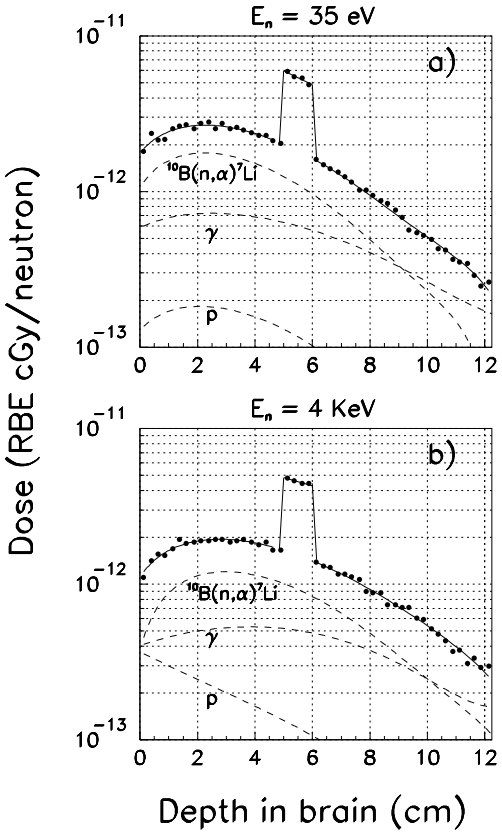


**Figure 1.** Depth-dose distribution in the brain for monoenergetic and unidirectional neutron beams of 35 eV (*a*) and 4 keV (*b*), simulated by means of a code based on the CERN library GEANT (the package MICAP is used for neutron transport). The symbols represent the results of the simulations, while the full curve shows the result of a fit of the depth-dose distribution performed with a fourth-order polynomial. The broken curves depict the contribution of the different reactions to the total dose. The comparison between the results at 35 eV and at 4 keV (in particular of the position and value of the maximum dose to healthy tissues) demonstrates the higher therapeutic efficacy of neutrons of few keV energy in the treatment of deep-seated tumours.

## 3. Figures of merit: results and discussion

In order to quantitatively determine the most appropriate neutron energy for the treatment of deep-seated tumours with BNCT, we have investigated several figures of merit. Figure 2 shows the advantage depth (AD) as a function of the neutron energy and blood $^{10}$B concentration, for a fixed tumour/blood ratio of $^{10}$B concentration. The advantage depth is defined as the depth at which the dose to tumour equals the maximum dose to normal tissues. As a general feature, AD seems to weakly depend on the $^{10}$B concentration, above 10 ppm. On the contrary, a strong dependence on the neutron energy can be observed in the figure. In particular, for all $^{10}$B concentrations, AD increases when going from thermal to epithermal neutrons, it reaches a maximum value for neutrons of a few keV, and then it sharply decreases for higher energies. The pronounced ridge in the few keV region represents a first indication of the optimal energy for the treatment of deep-seated tumours. More quantitative information can be obtained from

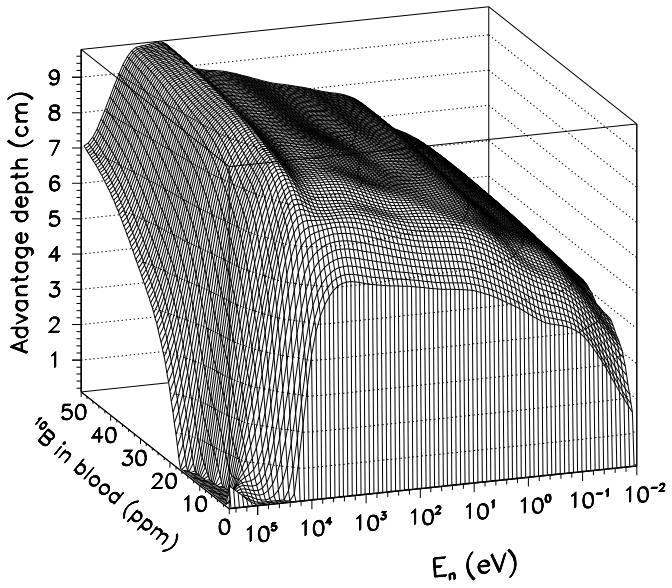


**Figure 2.** Advantage depth (AD) as a function of the neutron energy and of the $^{10}$B concentration in blood, as obtained from the simulations described in the text. A fixed value of 4.3 is assumed for the ratio of $^{10}$B concentrations in tumour and blood.

figure 3. In panel (*a*), AD is plotted for different neutron energies as a function of the $^{10}$B concentration in blood. As expected, AD saturates for concentrations above 10 ppm at all energies except for the 100 keV case. The saturation level strongly depends on the neutron energy, with the maximum value is reached around 10 keV. Above this region, the large dose released by recoil protons causes a sharp fall of AD, as can be clearly seen in figure 3(*b*), in particular for the realistic $^{10}$B concentration of 10 ppm.

To further characterize the optimal energy for the treatment of deep-seated tumours, we have analysed the therapeutic gain (TG), defined as the ratio between the average dose deposited in the tumour region and the maximum dose delivered to normal tissues. In analogy with charged particle therapy, this quantity may provide a more direct indication on the effectiveness of neutrons of a given energy in the treatment of deep-seated tumours. Furthermore, as will be shown later, the therapeutic gain allows us to easily estimate the quality of epithermal neutron beams of any energy spectrum, thus facilitating the comparison between different neutron sources.

To accurately determine the therapeutic gain from our simulations, we employ a fitting procedure on the Monte Carlo results. In particular, the dose distribution to healthy tissues is fitted using a fourth-order polynomial, up to 12 cm depth and excluding the tumour region; the results of the fit are shown by the continuous curves in figure 1. In the whole region considered in these simulations, i.e. for neutrons of 0.025 eV $< E_n <$ 1 MeV, a fourth-order polynomial accurately reproduces the behaviour of the depth-dose distribution. The maximum dose to normal tissues is then analytically determined from the result of the fit, while the average dose to tumour is obtained by integrating the dose over the tumour region. Since the dose distribution exhibits a slight but not negligible dependence on the depth over the size of the tumour, this choice provides an indication of the dose delivered to the whole tumour region.

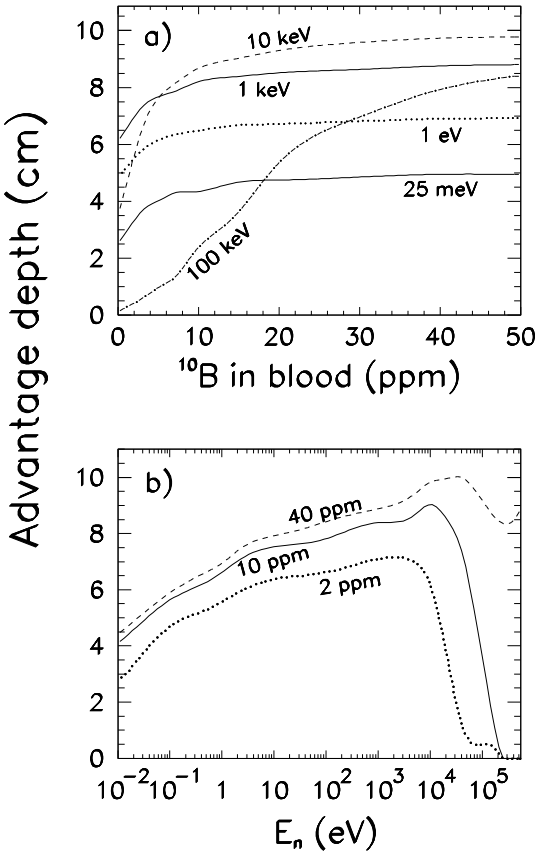


**Figure 3.** (*a*) Advantage depth (AD) as a function of $^{10}$B concentration in blood for some given neutron energies. (*b*) AD as a function of the neutron energy for some values of the $^{10}$B concentration in blood. A fixed value of the tumour/normal tissue concentration ratio of 4.3 is used in the simulations.

The analysis of the therapeutic gain versus the energy of the incoming neutron beam, at fixed tumour geometry and location, is shown in figure 4. In correspondence with the assumed $^{10}$B concentration and tumour depth, the therapeutic gain shows a sharp maximum between 1 and 10 keV. Neutrons of lower energies mainly thermalize before the tumour location, while for neutron energies in excess of a few tens of keV, the large dose to the skin and the brain surface produced by recoiling protons causes a fast drop in the therapeutic gain. For this reason, the optimization of the neutron beam is related, among other features, to the minimization of the high-energy component in the spectrum of the therapeutic neutron beam.

Although the exact value of the therapeutic gain depends on the RBE factor, on the $^{10}$B concentration and on the tumour depth, the evolution of TG as a function of the neutron energy is not expected to change dramatically in the range of values commonly considered for these parameters. In particular, a shift of the peak location towards higher neutron energies is observed for deeper tumours. The open symbols in figure 4 show the therapeutic gain as a function of neutron energy for a tumour located at midbrain, i.e. centred at 8 cm. In this case, the maximum value of TG is obtained for a neutron energy slightly above 10 keV.

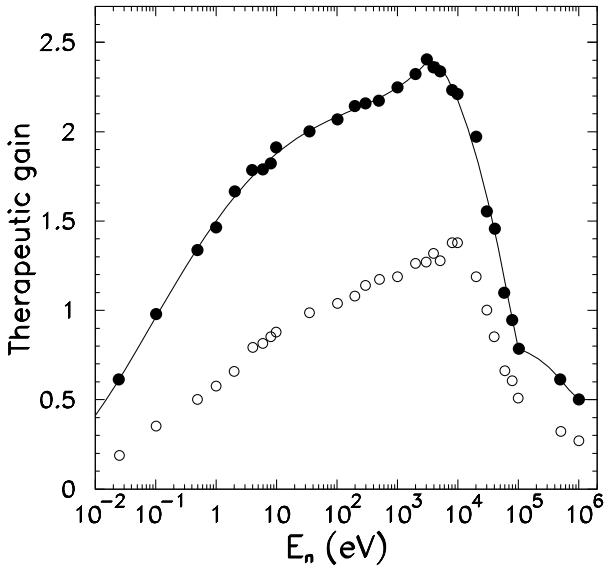


**Figure 4.** Therapeutic gain as a function of the neutron energy for a monoenergetic and unidirectional neutron beam. The full symbols represent the results of the simulations performed for several neutron energies between 25 meV and 1 MeV, for a tumour located at a depth of 5 cm inside the brain; the full curve represents the results of a fit performed with polynomials in three different ranges (25 eV $< E_n <$ 4 keV; 4 keV $< E_n <$ 100 keV; $E_n >$ 100 keV). The open symbols represent the results of the simulations for a tumour located at midbrain (depth of 8 cm).

## 4. A fast method for beam quality evaluation

The analysis of the therapeutic gain indicates that the treatment of deep-seated tumours would require monoenergetic neutron beams with an energy of a few keV. Realistically, however, neutron beams can only be produced with a composite energy distribution. Understanding the optimal features of real beams becomes necessarily more complicated. Lengthy and sophisticated Monte Carlo simulations of the dose distribution are commonly performed to assess the quality of different neutron beams or to find the beam-shaping assembly configuration leading to therapeutic beams of the desired quality. Here we propose a method that allows us to determine with a good approximation the quality of neutron beams of any energy profile, without performing a complete simulation of the dose distribution in the brain. Because of its simplicity and accuracy, this procedure can be useful for a systematic investigation of different moderator materials and geometry of a beam-shaping assembly, or to perform a quick comparison between neutron beams of known energy spectrum.

The method is based on the observation that the dose released by a neutron beam of composite energy spectrum can be decomposed into the contributions of the different energy components. An analytical expression of the dose distribution $D(E, x)$, as a function of the neutron energy $E$ and of the depth $x$, is obtained by fitting the dose distribution for monoenergetic beams in the variable $x$ using a fourth-order polynomial, and then expressing the coefficients of these polynomials as a function of the neutron energy, either by interpolation of by a fitting procedure. As previously mentioned, in the whole energy region considered in the simulations, i.e. for neutrons of 0.025 eV $< E_n <$ 1 MeV, the analytical representation of $D(E, x)$ closely reproduces the behaviour of the simulated dose distributions. The therapeutic

gain is also represented as a function of the neutron energy by means of a polynomial fit, whose result is shown by the curve in figure 4.

For a given normalized neutron spectrum $\mathrm{d}n(E)/\mathrm{d}E$, the overall dose distribution in healthy tissues is obtained by integrating $D(E, x)$ over the energy, weighted by the neutron energy spectrum:

$$D(x) = \int D(E, x) \frac{\mathrm{d}n(E)}{\mathrm{d}E} \mathrm{d}E. \tag{1}$$

In correspondence to the tumour location, the dose is calculated according to the energy-dependent therapeutic gain, $\mathrm{TG}(E)$, of figure 4, using the formula

$$D_T = \int \mathrm{TG}(E) D_m(E) \frac{\mathrm{d}n(E)}{\mathrm{d}E} \mathrm{d}E \tag{2}$$

where $D_m(E)$ is the maximum dose to the normal tissues for a given neutron energy $E$.

The procedure described above has been applied to the realistic case of an accelerator-based neutron source for BNCT using near threshold charged particle reactions (Harmon *et al* 1997). The histogram in figure 5(*a*) shows the energy spectrum of the epithermal neutron beam that would be obtained with the $^7$Li(p, n)$^7$Be reaction at $E_p = 1.95$ MeV. Neutrons emitted in this reaction were generated according to the cross sections of Liskien and Paulsen (1975), and moderated to a useful energy by a beam shaping assembly made of a BeO moderator 8 cm thick, a Pb reflector, a polyethylene collimator and a 1 mm thick $^6$Li layer for thermal neutron filtering. The resulting energy spectrum is obtained by recording the energy of neutrons impinging on a tally surface placed just outside the beam-shaping assembly.

The overall dose distribution corresponding to the spectrum of figure 5(*a*) is then calculated by applying the convolution method expressed by equations (1) and (2). The result is shown by the full curve in figure 5(*b*). The ratio of the tumour to normal tissue doses allows us to immediately calculate the corresponding overall therapeutic gain, which in this case is $\mathrm{TG} = 2.05$. For comparison, the symbols in the figure represents the results of a complete simulation of the dose deposition process, assuming a unidirectional neutron beam with energy distribution shown in figure 5(*a*).

The possibility of predicting the dose distribution and the overall therapeutic gain for neutron beams of any energy distribution, without performing lengthy simulations, is the great advantage of the method presented here. This is very convenient, in particular when performing a systematic analysis of the optimal beam-shaping assembly configuration. In this case, the final dose can be estimated from the neutron energy distribution after the moderator process, without the need to perform a dose calculation for each choice of beam-shaping assembly. The results of this method, however, represent only an approximation of the dose that can be obtained with a given neutron beam. The uncertainty connected to the fitting procedure can be estimated by comparing the predicted dose distribution (curve) with the results of the simulations of the dose, performed with a parallel neutron beam with the energy spectrum of figure 5(*a*) (shown by the symbols). The dose obtained with the convolution method is systematically lower, by $\sim$5%, relative to the simulated dose, while the two therapeutic gains differ by only $\sim$2%. A larger uncertainty, however, is associated with the assumption of unidirectionality, used in the present analysis of the dose distribution. In the real situation, therapeutic neutron beams are characterized by a large divergency, in particular if significant moderation and reflection processes are involved in their production. Furthermore, the reminiscence of the emission angular distribution for near-threshold reactions may cause a non-homogeneous neutron flux over the head surface, which may affect the dose distribution at depth in the brain. Although a precise determination of the dose corresponding to a given neutron source requires a complete simulation of the moderation and dose deposition process, the method presented here may

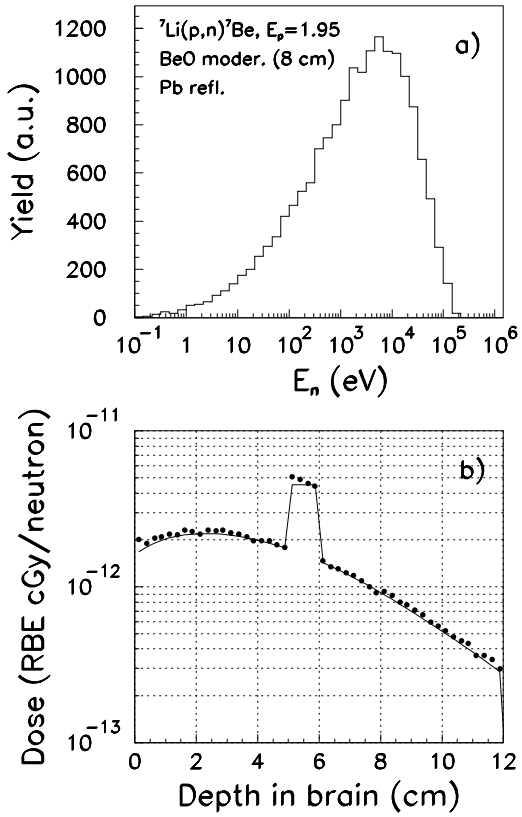


**Figure 5.** (*a*) Energy distribution of the epithermal neutron beam that can be obtained by moderating neutrons emitted in the $^{7}$Li(p, n)$^{7}$Be reaction at 1.95 MeV. The beam-shaping assembly chosen in this case consists of 8 cm BeO moderator, a Pb reflector, a polyethylene beam delimiter and a $^{6}$Li filter. The curve in (*b*) shows the depth-dose distribution produced by such a beam, as predicted from the convolution method described in the text. For comparison, the symbols show the results of a complete simulation of the dose produced in brain by a unidirectional neutron beam with the energy distribution as in (*a*).

be conveniently employed for a relative comparison between different BSA solutions. A refinement of the method with the inclusion of the effect of the beam divergence is currently being investigated.

## 5. Conclusions

The results of the simulations, performed for monoenergetic neutron beams over a wide energy range, have been analysed with the aim of characterizing the optimal neutron energy for the treatment of deep-seated tumours. The figures of merit considered here, the advantage depth (AD) and the therapeutic gain (TG), clearly indicate that the most useful neutrons for BNCT are those is in the region of few keV energy, for a 5 cm deep tumour and for realistic values of $^{10}$B concentrations and RBE factors.

The same figures of merit, and in particular the therapeutic gain, clearly indicate the need to minimize the contribution of fast neutrons ($E_n > 50$ keV) in the therapeutic beam, since

their presence is responsible for a large surface dose which poses some constraints on the dose that can be delivered to the tumour region. This conclusion is also valid for deeper tumours, such as the ones located at midbrain, although the maximum value of the therapeutic gain in this case is shifted towards higher neutron energies, slightly above 10 keV.

The results of the simulations for monoenergetic neutron beams have been extended to the more realistic case of therapeutic beams of composite energy spectrum, by means of a convolution method which relies on a fitting procedure and on a weighted integral of the doses to normal and tumour tissues. The method allows us to estimate the overall dose distribution and therapeutic gain without performing lengthy simulations of the neutron transport. Although such simulations are still necessary for an accurate determination of the dose distribution, the method can be conveniently applied to find the near-optimal material and geometry of the beam-shaping assembly for a given neutron source, or to perform a comparison between epithermal neutron beams obtained from different neutron-producing reactions.

## References


Aizawa O 1994 Evaluation of neutron irradiation field for boron neutron capture therapy by using absorbed dose in a phantom *Int. J. Radiat. Oncol. Biol. Phys.* **28** 1143–8

Allen D A and Beynon T D 1995 A design study for an accelerator-based epithermal neutron beam for BNCT *Phys. Med. Biol.* **40** 807–21

Allen D A, Beynon T D, Green S and James N D 1999 Toward a final design for the Birmingham boron neutron capture therapy *Med. Phys.* **26** 77–82

Barth R F, Soloway A H and Brugger R M 1996 Boron neutron capture therapy of brain tumors: past history, current status and future potential *Cancer Invest.* **14** 534–50

Bleuel D L, Donahue R J, Ludewigt B A and Vujic J 1998 Designing accelerator-based epithermal neutron beams for BNCT *Med. Phys.* **25** 1725–34

Briesmeister J F 1993 MCNP—a general Monte Carlo code for *N*-particle transport code 4A *Los Alamos National Laboratory Report* LA-12625-M

Brun R, Hansroul M and Lassalle J C 1986 GEANT3 *CERN Report* DD/EE/84.1

Coderre J A and Morris G M 1999 The radiation biology of boron neutron capture therapy *Radiat. Res.* **151** 1–18

Harmon J F, Kudchadker R J, Kunze J F, Serrano S W, Zhou X L, Harker Y D and Hamm R W 1997 Accelerator neutron sources for neutron capture therapy using near threshold charge particle reactions *Proc. 14th Int. Conf. on Applications of Accelerators in Research and Industry (AIP Conf. Proc. 392)* pp 1285–8

Johnson J O and Gabriel T A 1988 A user's guide to MICAP: a Monte Carlo ionization chamber analysis package *Oak Ridge National Laboratory Report* ORNL/TM-10340

Konijnenberg M W, Dewit L G H, Mijnheer B J, Raaijmakers C P J and Watkins P R D 1995 Dose homogeneity in boron neutron capture therapy using an epithermal neutron beam *Radiat. Res.* **142** 327–39

Liskien H and Paulsen A 1975 Neutron production cross-sections and energies for the reactions $^{7}$Li(p, n)$^{7}$Be and $^{7}$Li(p, n)$^{7}$Be* *At. Data Nucl. Data Tables* **15** 57–84

Liu H B, Greenberg D D, Capala J and Wheeler F J 1996 An improved neutron collimator for brain tumour irradiations in clinical boron neutron capture therapy *Med. Phys.* **23** 2051–9

Nigg D W 1992 Three-dimensional radiation dose distribution analysis for boron neutron capture therapy *Nucl. Sci. Eng.* **110** 16–31

——1994 Methods for radiation dose distribution analysis and treatment planning in boron neutron capture therapy *Int. J. Radiat. Oncol. Biol. Phys.* **28** 1121–34

Wallace S A, Mathur J N and Allen B J 1994 Treatment planning figures of merit in thermal and epithermal boron neutron capture therapy of brain tumours *Phys. Med. Biol.* **39** 897–906

Wheeler F J, Nigg D W, Capala J, Watkins P R D, Vroegindeweij C, Auterinen I, Seppala T and Bleuel D 1999 Boron neutron capture therapy (BNCT): implications of neutron beam and boron compound characteristics *Med. Phys.* **26** 1237–44

Yanch J C, Zhou X L and Brownell G L 1991 A Monte Carlo Investigation of the dosimetric properties of monoenergetic neutron beams for neutron capture therapy *Radiat. Res.* **126** 1–20

Zamenhof R, Redmond E, Solares G, Katz D, Riley K, Kiger S and Harling O 1996 Monte Carlo-based treatment planning for Boron neutron capture therapy using custom designed models automatically generated from CT data *Int. J. Radiat. Oncol. Biol. Phys.* **35** 383–97